

## Chapter 4.6

# JOINING FRAGMENTED MARBLE ARCHITRAVES USING TITANIUM BARS: A NUMERICAL ANALYSIS

Stavros K. Kourkoulis<sup>1</sup>, Evi Ganniari-Papageorgiou<sup>1</sup> and Marilena Mentzini<sup>2</sup>

<sup>1</sup>*School of Applied Sciences, Department of Mechanics, National Technical University of Athens, Theocharis Building, 5 Heroes of Polytechnion Avenue, 157 73 Zografou, Athens, Hellas, stakkour@central.ntua.gr;* <sup>2</sup>*Committee for the Conservation of the Acropolis Monuments, Acropolis, Athens, Hellas*

**Abstract:** The problem of joining together fractured marble architraves is studied numerically in the present paper using the Finite Element Method. The study was motivated by the needs of the conservation project in progress of the Parthenon Temple on the Acropolis of Athens, where pioneering work is carried out during the last thirty years concerning, among others, the restoration of fragmented architraves using titanium bars. The numerical model constructed simulates the bending test of a centrally fractured prismatic marble architrave of rectangular cross section. The influence of the loading mode simulating the actual loading conditions is explored and the distribution of the stress and strain components is investigated in an effort to detect the points most prone to fail.

**Key words:** natural building stones; marble; Dionysos marble; restoration; monuments; architraves; bending; titanium; finite element method.

## 1. INTRODUCTION

The durability of interventions and the protection of the authentic material during the restoration of a monument are among the priorities of scientists working in relevant projects. The experience of previous botched restoration attempts pressed upon a thorough study of the materials used and their compatibility (both mechanical and physico-chemical) with the authentic one. In this direction the scientists working for the restoration of the monuments on the Acropolis of Athens have developed a pioneering method for joining together fragmented structural elements using titanium bars<sup>1-3</sup> in combination

with suitable cement mortar. The final target is to reach either the initial load-carrying capacity of the member (if it is possible) or the capacity corresponding to the maximum load expected to be exerted on the particular member after the completion of the project (taking into account all possible future interventions). The latter is the approach preferred when the reinforcing titanium bars required for reaching the initial carrying capacity can not be fitted either due to the shape of the sections of the members or due to the relatively small size of the remaining authentic parts of the member or due to the great loss of authentic material<sup>3</sup>. The above method is nowadays used widely for the restoration of multi-fragmented architraves (epistyles) of the monument, which are subjected principally to bending by distributed loads due to their own weight and the weight of the superimposed structural elements.

The experimental assessment of the reinforcing method requires carefully designed and executed laboratory bending experiments. Unfortunately these tests are usually carried out as either three- or four-point bending, since the simulation of a uniformly distributed loading is not easily realizable for the majority of the laboratory loading frames, unless dead-weight type loads are used. However, even the latter procedure is difficult in case large specimens are to be tested in order to take into consideration the size effect (extremely pronounced for geomaterials and especially for marble) shadowing the experimental results if relatively small scaled specimens are used.

Recently a multi-point bending arrangement (Figure 1) was designed approaching in a better manner the uniformly distributed load<sup>4,5</sup>. The arrangement was used in bending experiments with specimens simulating in an 1:3 scale typical fragmented architraves of the Parthenon Temple, in an effort to

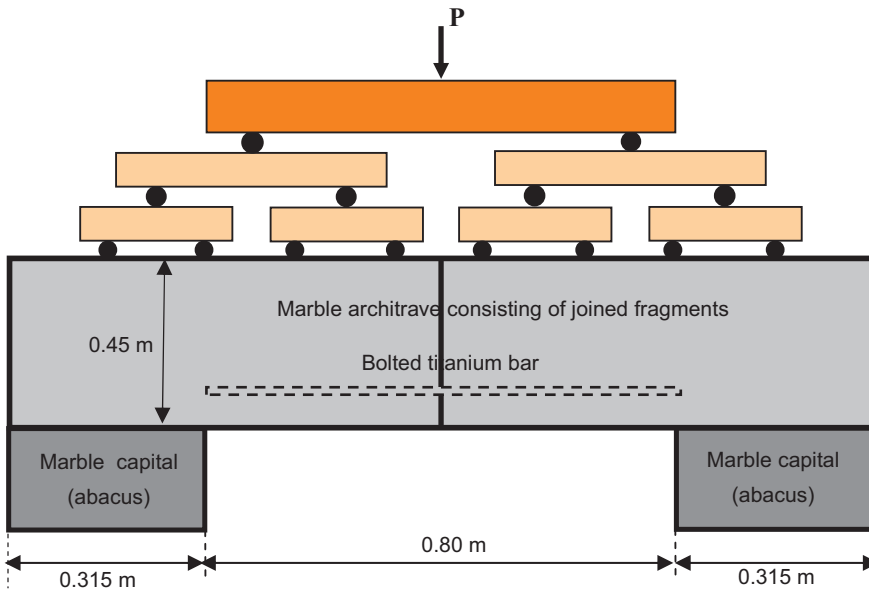


Figure 1. Schematic representation of the arrangement modeled numerically.

assess the reinforcing method of the architraves. The analysis of the results of the tests revealed some discrepancies between them and the respective ones obtained from the theoretical analysis<sup>6</sup>. It was thus indicated that one should consider carefully both the loading system as well as the details of the supports on which the specimen rests, in order to determine the actual span of the architrave and therefore the maximum developed bending moment.

In this sense a numerical analysis is carried out in the present paper divided into two parts: In the first part the possible ways of simulating the actual loading conditions during a typical bending test is studied and the one producing the most severe stress field is pointed out. For the sake of simplicity and CPU-time economy the analysis in this part is carried out considering an intact architrave. In the second part the stress and strain fields developed in a prismatic architrave consisting of two equal fragments joined together with one titanium bar are explored in case the specimen is loaded according to the loading way producing the most severe stress field, as it has been determined in the first part of the study.

## **2. BENDING UNDER HOMOGENEOUS LOAD**

### **2.1 Bending of intact marble architraves**

The influence of the exact load-application mode on the stress distribution during the bending test of an intact marble architrave was studied numerically using the Finite Element Method with the aid of the commercially available software ANSYS 9.0. The geometry of the model matched exactly that of the worst damaged architrave of the north colonnade of the Parthenon Temple, i.e the fifth external one, in a scale of 1:3 (ignoring damages and cracking).

The mechanical properties assigned to the material were those of the Dionysos marble, since it is used extensively for the construction of copies of lost members or of completions of damaged ones by the experts working for the restoration of the Temple. The material was considered as linearly elastic and isotropic with Young's modulus  $E_m=70$  GPa, Poisson's ratio  $\nu_m=0.3$ , density  $\rho_m=2.78$  gr/cm<sup>3</sup> and coefficient of static friction  $m=0.70$ . The transverse isotropy of Dionysos marble and its slight non-linearity<sup>7</sup> were ignored.

The dimensions of the scaled model are: Length  $L=1.43$  m, thickness  $w=0.18$  m and height  $h=0.45$  m. The span was set equal to  $s=0.80$  m.

Four loading types were simulated:

- Uniformly distributed load along the total length (Figure 2a).
- Uniformly distributed load along the span (Figure 2b).
- Eight-point bending along the span (Figure 2c).
- Eight-point bending along the total length (Figure 2d).

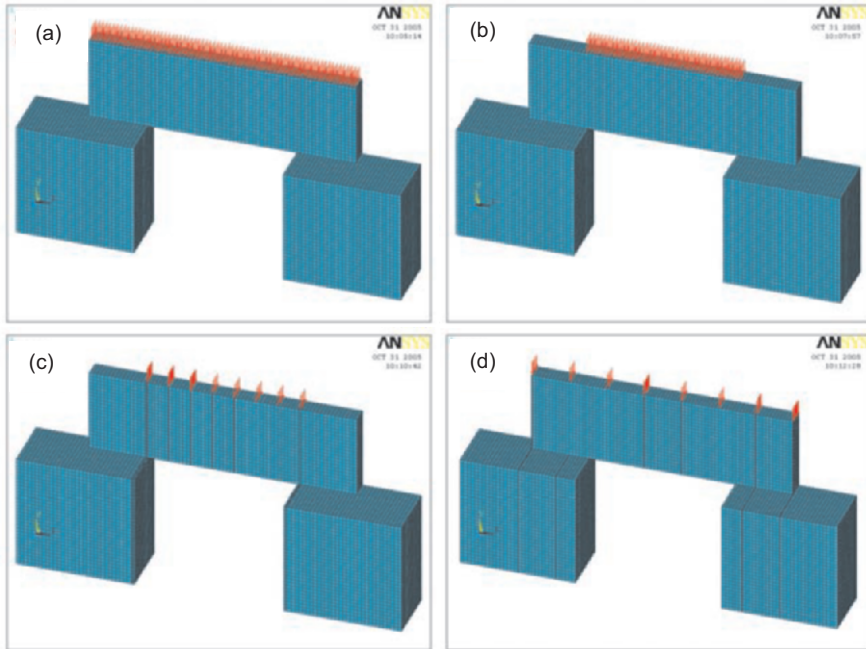


Figure 2. The four loading cases studied numerically.

Both the architrave and the abacuses (capitals) on which it rests were taken into consideration and thus the numerical model constructed consisted of three volumes of the same material, as it can be seen in Figures 1 and 2.

The mapped meshing technique was chosen. Mapped mesh consists of either all quadrilateral or all triangular elements. The volume was shaped as a brick (bounded by six areas) and the element used was the SOLID185, defined by eight nodes with three degrees of freedom at each one. Concerning the density of the mesh it is known that it plays a significant role in obtaining accurate results from a numerical analysis. Several preliminary “runs” were made with different element sizes and it was concluded that for meshes with 50000 elements and over the results converge in a satisfactory manner.

Two couples of 2-D contact elements were introduced between the architrave and the abacuses. For the needs of the present study rigid-rigid contact was assumed since the contact surfaces are made from the same material. The TARGE170 and the CONTA174 elements were used for the analysis. For the quantification of the “contact element stiffness” additional preliminary “runs” indicated that for values exceeding 20 the results are stabilized.

Concerning the boundary conditions it was assumed that the lower bases of the supporting abacuses are rigidly clamped. For reduction of the “running-time” advantage was taken of the vertical plane of symmetry including the axis of the architrave and only half of the configuration was modelled (see Figure 2). The total load exerted was equal to 65 kN, i.e. the maximum load expected for the particular architrave, after the completion of its restoration.

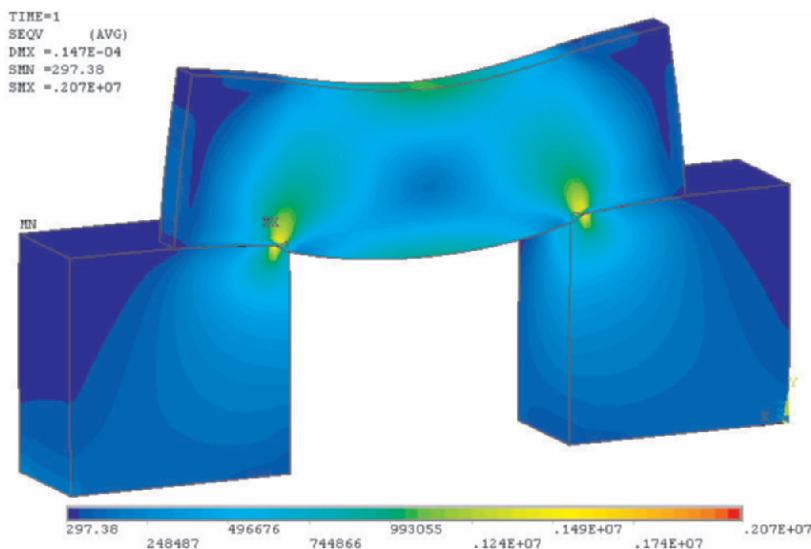


Figure 3. The distribution of the von Mises equivalent stress for the maximum load expected.

Typical results of the analysis are shown in Figure 3, in which the distribution of the von Mises equivalent stress for the whole model is plotted for the second loading type. It is observed that the maximum stress is developed at points close to the corners (fillets, “*hypotomess*”, *υποτομές*) of the supporting abacuses rather than at the mid-span, as it was perhaps expected. The qualitative behaviour of the stress field for the other loading types is of similar nature.

The variation of the equivalent stress along the central longitudinal line of the lowest base of the architrave is plotted in Figure 4 for all four loading types. The conclusions concerning the dramatic influence of the corners of the abacuses on the stress field in the architrave are verified quantitatively: The stress at the mid-span of the architrave is in all cases almost 70% lower compared to the stress developed in the vicinity of the corners of the abacuses. It is obvious that unless the corners are rounded the failure of the architrave will start there either as local exfoliation or cracking. This conclusion was recently supported by a thorough in situ observation of the architraves of the Parthenon Temple, which have never been removed from their original place from the antiquity until the present days: More than half of the fractures and the cracks observed (excluding the ones caused by interventions) have their starting points very close to the vicinity of the corners of the abacuses<sup>6</sup>.

From Figure 4 it is also concluded that the most intensive stress fields developed at the central cross section of the architrave are those of cases (b) and (c), i.e. when the load is restricted in the span of the member instead of its total length. However, the most striking conclusion is that in case the load is uniformly distributed the maximum stress is slightly higher compared to the respective case where the load is concentrated at eight strips. On the other hand the loading type causing the weakest stress field is the eight-point

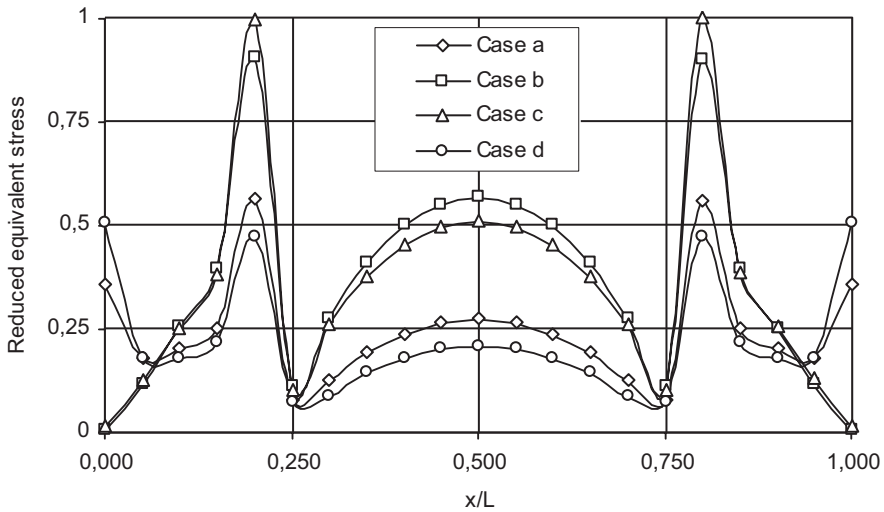


Figure 4. The equivalent von Mises stress along the bottom central longitudinal line of the architrave for the four loading cases. The distance is reduced over the length,  $L$ , of the architrave while the stress is reduced over the maximum value developed.

bending with strip loads applied along the whole beam length. It is thus indicated that the simulation of bending under uniform load with multi-point bending tests leads to underestimation of the actually developed stress field.

## 2.2 Bending of a fragmented and restored architrave

As a next step a symmetrically fractured and restored architrave is considered. The architrave simulates again the fifth external architrave of the north colonnade of the Parthenon Temple in a scale of 1:3. The reinforcement required for the restoration was calculated according to a recently developed method<sup>2,3</sup> which is described shortly in the next paragraph.

### 2.2.1 The calculation of the reinforcement required

The procedure followed here was introduced by Ioannidou and Paschaliades<sup>2</sup> and Mentzini<sup>3</sup> for the needs of the extensive restoration project in progress of the Acropolis of Athens monuments. The architraves are simulated as composite structural members made of marble and titanium bars subjected to simple bending. The analysis is based on the following assumptions:

- The stresses developed do not exceed the linearity limit of the materials.
- Marble is assumed as transversely isotropic material, the modulus of elasticity of which is constant within the bedding planes.
- The strains developed are compatible to each other; there is no relative sliding or pull-out of the reinforcing bars from the marble body.
- The bending loads act normally to the bedding planes.

- The cross sections remain plane and normal to the longitudinal neutral axis of the beam (Bernoulli-Euler technical beam-bending theory).

The latter is perhaps the weakest assumption of the method since the ratio of the length over the height of most architraves of the monument is far from 10, the conventional limit of validity of the Bernoulli-Euler technical theory.

The approach takes into consideration all the loads that could be applied on the member after it is replaced in its initial position in the restored monument. These loads include the own weight of the member, the weights of the members that will rest on it after the restoration as well as possible dynamic loads (earthquake loading). The latter are taken into account by increasing the respective static loads using suitable safety factors.

As a simple example consider an architrave of rectangular cross section reinforced with a single titanium bar. The moment,  $M_{ex}$ , developed by the action of the externally applied loads is undertaken by an internal couple of forces, compressive in the marble and tensile in the titanium bar. Denoting by  $A_t$  the cross section area of the titanium bar, by  $\epsilon_m$  and  $\epsilon_t$  the strains in marble and titanium, by  $\sigma_m$  and  $\sigma_t$  the stresses in the uppermost fiber of the marble and in the titanium bars, by  $E_m$  and  $E_t$  the elasticity moduli of marble and titanium, respectively, and finally by  $F_t$  the force exerted by the titanium bar (Figure 5), Hooke’s law and the strain compatibility condition give:

$$\epsilon_m = \frac{\sigma_m}{E_m}, \quad \epsilon_t = \frac{\sigma_t}{E_t} \Rightarrow \frac{\epsilon_m}{\epsilon_t} = \frac{E_t}{E_m} \frac{\sigma_m}{\sigma_t} \tag{1}$$

$$\frac{\epsilon_m}{\epsilon_t} = \frac{y_{na}}{h_t - y_{na}} \tag{2}$$

Combining Eqs.(1) and (2) one obtains:

$$\sigma_m = \frac{y_{na} E_m}{(h_t - y_{na}) E_t} \sigma_t \tag{3}$$

where  $y_{na}$  and  $h_t$  are the distances of the neutral axis and the titanium layer from the upper side of the beam, respectively. Denoting by the lever of the internal couple of forces and by  $b$  the width of the cross section of the architrave, the equation of equilibrium of moments yields:

$$\sigma_m \frac{y_{na} b}{2} z = F_t z = \sigma_t A_t z \tag{4}$$

Combining Eqs.(3) and (4) one obtains a simple second order algebraic equation, which if solved for  $y_{na}$  gives the position of the neutral axis as:



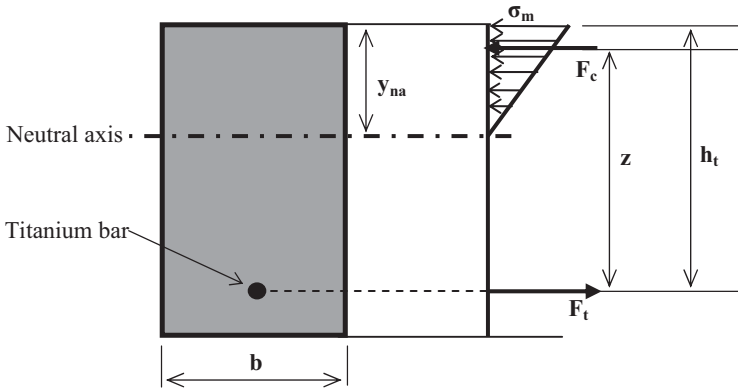


Figure 5. Reinforcing an architrave using one titanium bar.

$$y_{na} = \frac{E_t A_t}{E_m b} \left[ -1 \pm \sqrt{1 + \frac{E_m 2bh_T}{E_t A_t}} \right], \quad 0 < y_{na} < h_T \quad (5)$$

Knowing  $y_{na}$  one can calculate the normal stresses developed in marble and titanium and compare them with the respective allowable ones.

### 2.2.2 Simulation of the bending of a restored architrave

The architrave was assumed to consist of two equal parts joined together with a single titanium bar, as shown schematically in Figure 1. The area of the cross section of the bar was determined according to the above procedure and its radius was found equal to  $r_t=12.7$  mm. The bar is placed at a distance  $h_t=0.305$  m from the upper side of the architrave. The length of the bar used was  $L_t=0.8$  m. The layer of cement used for increased adhesion was ignored.

The mechanical properties of marble are the same with the respective ones of the intact architrave while these assigned to the titanium bar were: Young's modulus  $E_t=105$  GPa, Poisson's ratio  $\nu_t=0.32$ , and density  $\rho_t=4.51$  gr/cm<sup>3</sup>.

The dimensions of the scaled model are again: Length  $L=1.43$  m, thickness  $w=0.18$  m and height  $h=0.45$  m. The span was set equal to  $s=0.8$  m.

The specimen was discretized without employing the mapped meshing technique. Instead attention was paid for suitable specification of divisions and spacing ratios on unmeshed lines. The mesh was denser in the vicinity of the titanium reinforcement as well as in the contact section of the two parts of the architrave. The SOLID187 element was used for the mesh. It is a tetrahedral structural solid defined by 10 nodes having three translational degrees of freedom at each node along the nodal  $x$ ,  $y$  and  $z$  directions. It has a quadratic displacement behaviour and it is well suited for irregular meshes. The final model consisted of 79596 such elements. An overall view of the model (architrave, supporting abacuses and titanium bar) is shown in Figure 6.



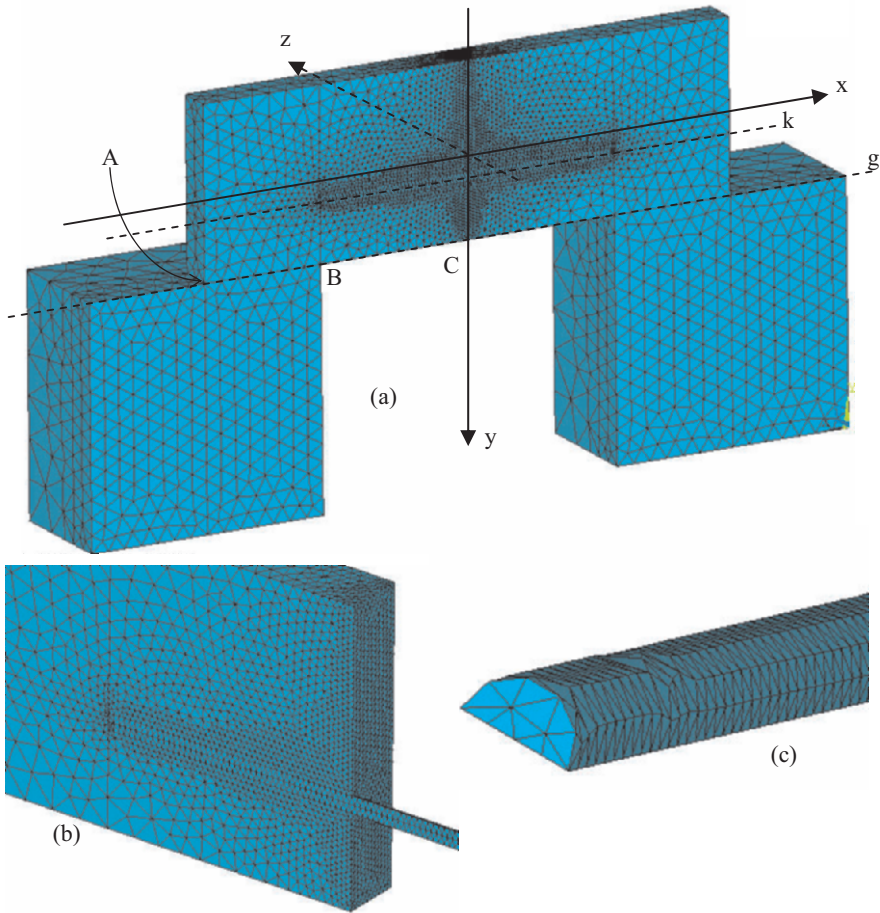


Figure 6. (a) An overall view of the model in the case of a fractured and restored architrave. (b) Detailed view of the mesh in the region of the titanium bar. (c) The mesh of the bar.

As it is seen from Figure 6 advantage was taken again of the vertical plane of symmetry containing the longitudinal axis of the architrave.

The load was simulated as uniformly distributed along the span of the architrave (case b), since according to the analysis of the previous paragraph, it corresponds to the worst case concerning the severity of the stress field developed. The total magnitude of the load exerted was again equal to 65 kN.

An overall view of the distribution of the von Mises equivalent stress in the case of the restored architrave is shown in Figure 7. As expected the situation is completely different compared to that of the intact member. The major part of the architrave is relieved and only at the region around the titanium bar the stresses approach the fracture stress of marble (~6-8 MPa), remaining however far from the respective limit of titanium (~300 MPa). Therefore the failure of the element in its restored form is expected around the section of the titanium in the cracked surface bar rather than at the abacuses' corners.

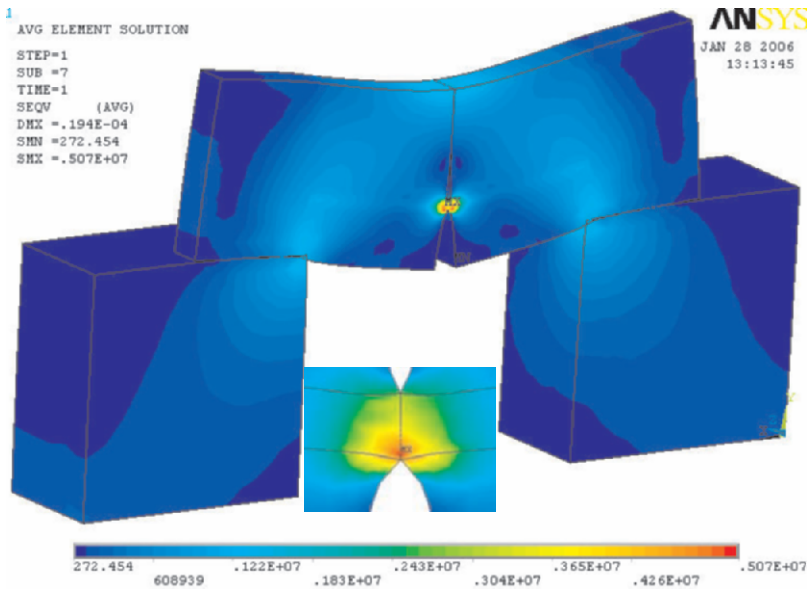


Figure 7. The distribution of the equivalent stress in the restored architrave. The embedded figure shows a detail of the central section around the titanium bar.

Some interesting conclusions can be drawn from Figure 8 in which the variation of the normal axial strain  $\epsilon_{xx}$  is plotted along the central vertical line of the cross section (axis  $y$ ) of the architrave. Axis  $y$  is reduced over the height of the beam,  $h$ , it is directed downwards and its origin corresponds to the geometrical center of the cross section (Figure 6). Concerning the intact member it is seen that the strain variation is not linear, as it is predicted by the classical Bernoulli-Euler technical bending theory, but rather it is of sigmoid nature. In addition the neutral axis does not pass from the centroid of the section: It is displaced downwards by more than 20% of the height. The

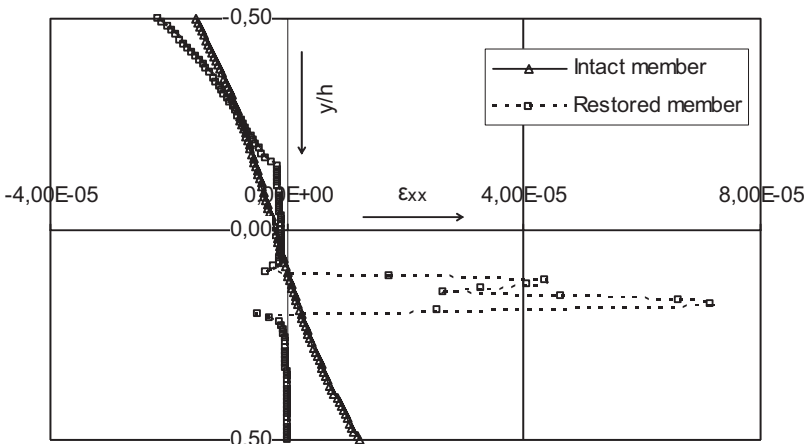


Figure 8. The variation of the axial strain  $\epsilon_{xx}$  along the height of the architrave.

above observations are in full agreement with the respective ones by Vardoulakis et al.<sup>8</sup> and Kourkoulis et al.<sup>9,10</sup>, who have pointed out experimentally both the lack of linearity of the strain variation as well as the displacement of the neutral axis again for Dionysos marble. Obviously these phenomena are attributed to the geometry of the architrave: The length over the height ratio is 3.2, far from the validity limit of the technical bending theory.

Concerning the variation of  $\epsilon_{xx}$  along the height of the restored architrave it is seen from the same figure that for the upper one third of the section the values are of the same sign and order of magnitude with those of the intact member. However, as one approaches the titanium bars the situation changes dramatically and the strain is almost zeroed since the contact of the two parts of the architrave is lost as it was seen in Figure 7. Then in the immediate vicinity of the reinforcing bar the strain attains tensile values almost ten times higher in comparison to the maximum one developed in the intact member. From this point on the strain becomes zero since below the reinforcement the contact of the two constituent parts is lost again. In any case, since the maximum fracture strain of Dionysos marble is about  $200 \mu\text{strain}$ <sup>7</sup> it is concluded that even in the region of the titanium bar the member is safe.

In Figure 9 the variation of the components of the displacement vector are plotted along the height of the architrave. As it is seen from Figure 9a the vertical displacement,  $u_y$ , in the restored case is almost constant (non-zero) all along the height of the member, although it appears to increase slightly in the portion below the reinforcing bar. On the contrary, for the intact member, the vertical displacement decreases almost linearly from a maximum value at the upper side of the architrave to a zero one at the bottom side, as it is predicted by the classical approach, since this side is load free. On the other hand the horizontal displacement,  $u_x$ , for the intact member is zero all along the height of the section as it was expected for obvious symmetry reasons.

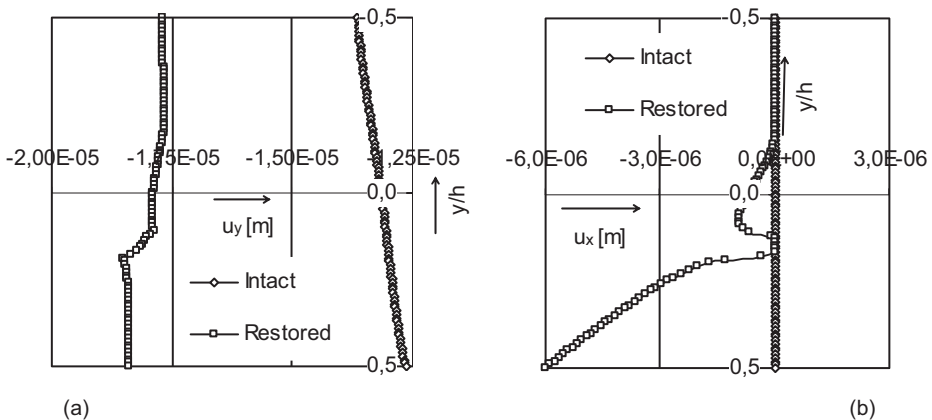


Figure 9. The variation of the vertical (a) and the horizontal (b) displacements along the height of the architrave at its central cross section.

This is not the case for the restored member for which  $u_x$  attains high values in the portions of the section where the contact of the two constituent parts is lost (both below and above the reinforcing titanium bar).

The variation of the normal components of the stress field along a horizontal line at the height of the axis of the reinforcing bar (line k in Figure 6) is plotted in Figure 10. For the intact member, the longitudinal stress,  $\sigma_{xx}$ , is almost zero, since by coincidence it is located, very closely to the displaced neutral axis of the architrave, as it was indicated from the analysis of Figure 8. For the restored member,  $\sigma_{xx}$  starts increasing abruptly as one approaches the central section and reaches a value of about 6 MPa, which is almost two orders of magnitude higher compared to the respective stress of the intact member. The behaviour of the transverse normal stress,  $\sigma_{yy}$ , is strongly influenced by the type and the size of the supporting abacuses: Indeed, for the portion of the architrave resting on them, relatively high compressive stresses appear, which for the intact beam tend to be eliminated towards the central section. At the same section of the restored member  $\sigma_{yy}$  becomes tensile with values equal to about 3 MPa, well comparable to the respective axial ones.

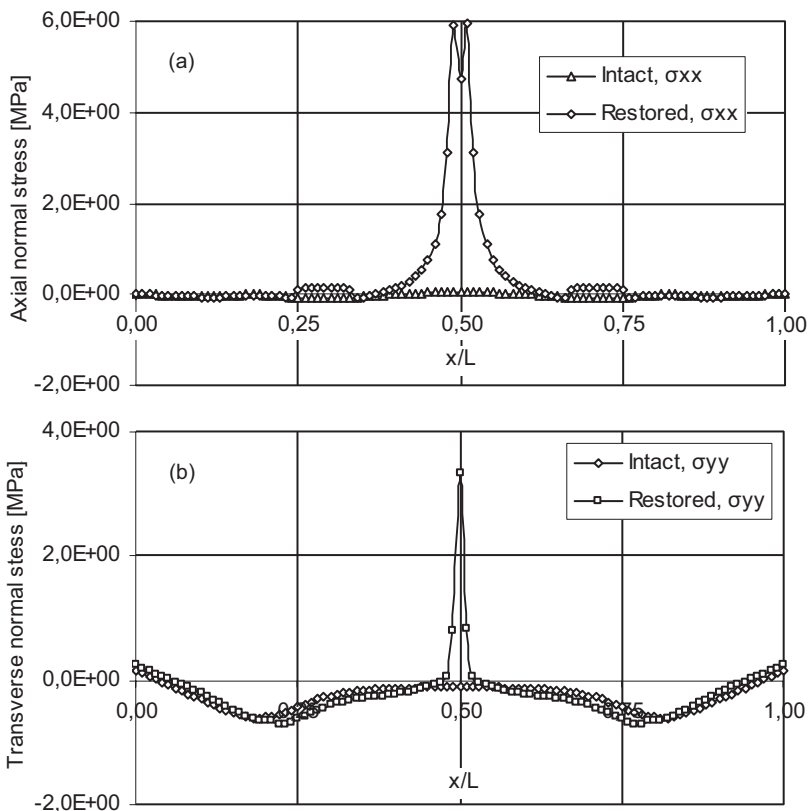


Figure 10. The variation of the normal axial,  $\sigma_{xx}$ , (a) and the normal transverse,  $\sigma_{yy}$  (b) stresses along an axial line (line k in Figure 6) passing from the center of the reinforcing bar.

As a last step of the investigation of the stress field the equivalent stress,  $\sigma_{eq}$ , is plotted in Figure 11 along the bottom central axial line (line g in Figure 6) of the member. As it was expected the equivalent stress along the span of the restored architrave is considerably lower in comparison to that in the intact member and (as it is expected) it becomes zero at the central section. At the points close to the corners of the abacuses the situation is reversed and the values of  $\sigma_{eq}$  are almost double with respect to those of the intact architrave. However, even at these points the stress field is weaker from that developed in the immediate vicinity of the titanium bar (Figure 10) indicating that in the case of a member restored with a single titanium bar failure is expected in the vicinity of the reinforcement while for the respective intact member failure is expected at the area of the corners of the abacuses supporting the epistyle. In order to avoid such failure phenomena ancient Greek engineers used to sculpture the so-called fillet (“*hypotomi*”, “*υποτομή*”) at the corners of the abacuses (capitals) supporting the epistyles (architraves), reducing the stress singularity and therefore the intensity of the stress field.

The variation of the axial strain  $\epsilon_{xx}$  along the same line g is shown in Figure 12. It is interesting to observe that in both cases (intact and restored) the axial strain obtains negative (compressive) values as one moves from point  $(x,y,z)=(-L/2, h/2, 0)$  (point A in Figure 6) towards the corners of the abacus (point B in Figure 6). The extreme values are about  $-20 \mu\text{strain}$  for the intact and  $-35 \mu\text{strain}$  for the restored member. This behaviour could be explained by taking into account the fact that part of the beam, initially resting on the abacuses, tends to lift up losing contact if the load is applied only along the span of the member<sup>4</sup>. From point B on the strain starts increasing in an almost parabolic form until it either reaches the maximum value at the mid-span of the intact beam ( $\sim 15 \mu\text{strain}$ ) or it becomes zero (restored member).

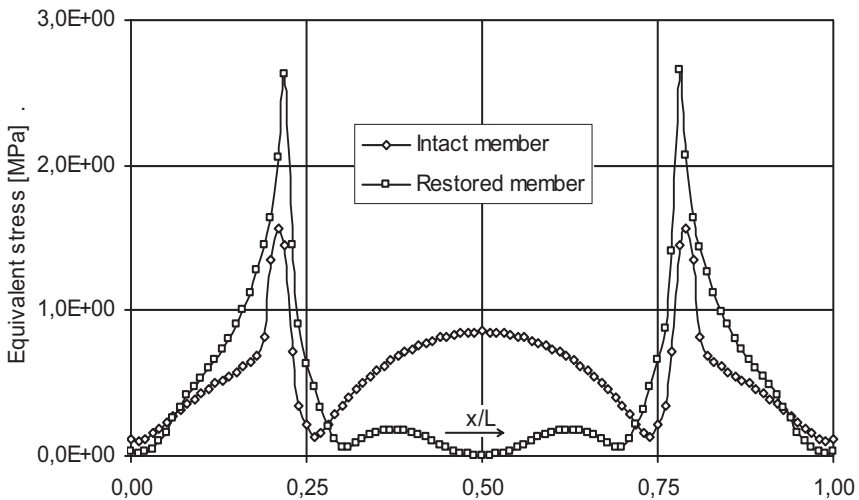


Figure 11. The equivalent stress along the bottom central axial line (line g in Figure 6).

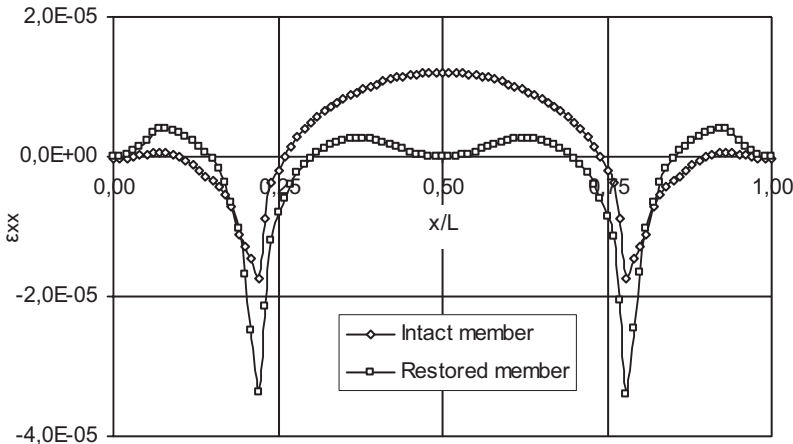


Figure 12. The axial strain  $\varepsilon_{xx}$  along the bottom central axial line (line g in Figure 6).

### 3. MULTI-POINT BENDING OF A RESTORED ARCHITRAVE

As it was mentioned in the introductory paragraph the realization of a bending test under homogeneous load is a difficult experimental task. Instead multi-point bending tests are carried out, as it was shown schematically in Figure 1. It is clear, however, that the stress and strain fields in the two cases are not equivalent, and as it has been proved<sup>4</sup> it is possible that multi-point bending results to weaker fields. Something like that, however, may be catastrophic if the design of the restoration is based on the results of the tests. In this direction the multi-point bending test of Figure 1 is studied here numerically for the same as previously restored architrave, in an effort to quantify a “loading-type” correction factor that could enable calibration of the experimental results, in order for them to be compatible with the theoretical ones.

The boundary conditions are the same as the ones described in paragraph 2.1 while the mesh is denser than that in paragraph 2.2.2. The load was again equal to 65 kN and it was divided in eight linear strip loads along the thickness of the beam. The strips were considered to be at equal distances from each other; the first one was exerted at a distance 0.09 m from the upper left edge. The width of each strip was set equal to 2 mm following the results of a recent analysis concerning the influence of the strip width on the overall strain field. The arrangement simulated the experimental set-up that will be used in future steps for the validation of the numerical model and the assessment of the method used for the calculation of the reinforcement required.

The results of the numerical analysis concerning the variation of the axial strain along the height of the architrave at the central section are plotted in Figure 13. In this figure the variation of  $\varepsilon_{xx}$  is plotted for both the intact and

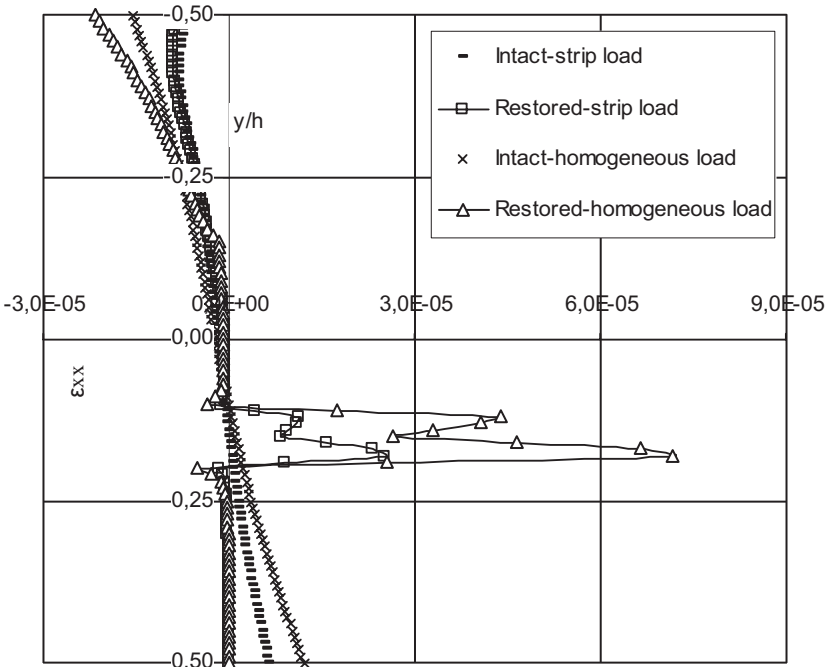


Figure 13. The variation of the axial strain,  $\epsilon_{xx}$ , along the height of the central cross section for both the intact and the restored architrave for uniform load and eight-point bending.

the restored architraves under either homogeneous load or eight-point bending, for comparison reasons. As it can be seen, the variation of  $\epsilon_{xx}$  for the intact member is again non-linear. It is clearly of sigmoid nature, obviously for the same reasons analysed in paragraph 2.1. Also, the neutral axis appears to be displaced downwards with respect to the longitudinal centroidal axis of the architrave. In addition, it is interesting to observe that the absolute values of the maximum strains attained at both the upper and the lower side of the beam are significantly higher in the case of the homogeneous load (compared to the respective values for multi-point bending). The same conclusions are valid for the restored architrave: The homogeneous load induces higher compressive strains (by about 30%) at the upper side of the member and, also, higher tensile strains (almost by 300%) in the vicinity of the reinforcing bar.

The variation of the axial strain along the bottom central line of the architrave is plotted in Figure 14 for both the homogeneous load and the eight-point bending. From a qualitative point of view, the graphs are of the same nature, but the absolute values of the axial strains in the vicinity of the corners of the abacuses for the case of eight-point bending are almost half the respective ones for bending under uniform load. The conclusions drawn for the variation of the equivalent stress, plotted in Figure 15, are almost identical: The stresses developed in the member subjected to bending under uniform load are almost two times higher compared to the eight point bending.



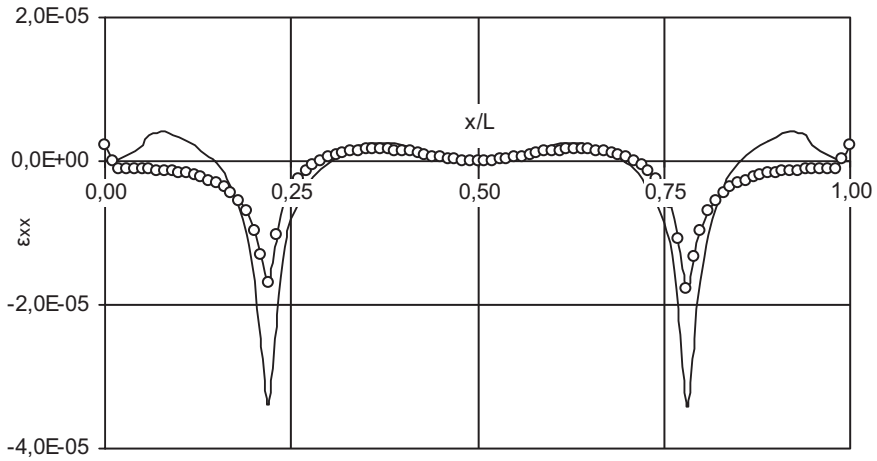


Figure 14. The variation of the axial strain along the bottom central line of the architrave. The continuous line corresponds to the homogeneous load while the one with the cyclic symbols to the eight-point bending.

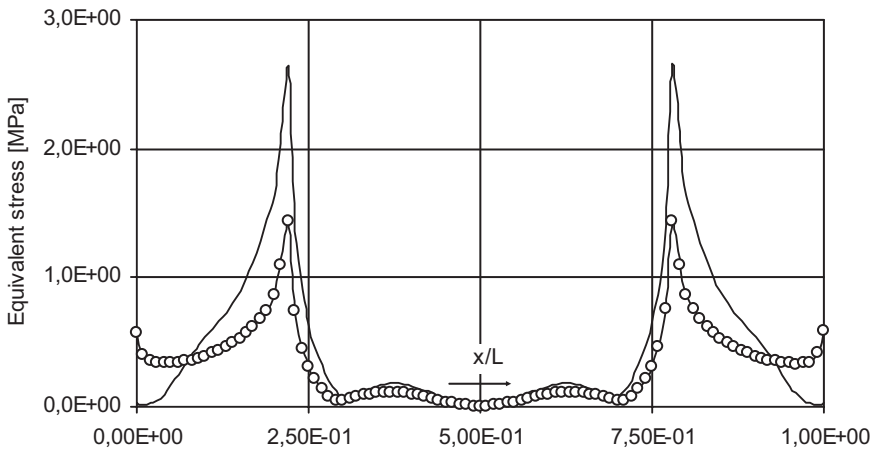


Figure 15. The variation of the equivalent stress along the bottom central line of the architrave. The continuous line corresponds to the homogeneous load while the one with the cyclic symbols to the eight-point bending.

#### 4. CONCLUSIONS

The restoration of a symmetrically fragmented architrave was explored numerically in the present study. The reinforcement required for joining together the parts of the member was calculated according to the method followed by the scientists working for the restoration of the Parthenon Temple on the Acropolis of Athens. The analysis revealed some critical points that

should be considered carefully before the design and the realization of interventions, at least on structural members carrying bending loads:

The calculation of the reinforcement is usually carried out adopting the technical bending theory (Bernoulli-Euler), which is approximately valid for relatively long beams. Most architraves, however, do not fulfill this requirement. As a result the axial strains are not distributed linearly along the height of the element but rather they follow a sigmoid distribution. In addition, the neutral axis is translated towards the bottom side of the architrave, rendering the calculations carried out considering the centroidal longitudinal axis as the neutral one rather rough approximations of the real conditions.

The points most prone to fail are the ones closest to the corners of the supporting abacuses rather than those at the mid-span of the beam, in case the architrave is intact. Such conclusion dictates that these corners should be rounded in order to prevent local exfoliations and cracking. On the contrary, in case the architrave is restored the points more prone to fail are the ones in the immediate vicinity of the reinforcing titanium bar.

The reproduction of actual bending conditions in the laboratory does not give reliable results unless the load was applied in exactly the same manner as it is applied in the real structure. More specifically the simulation of bending under uniform load by a laboratory multi-point bending test does not lead to accurate results unless the loading points are too many, something unrealizable for practical reasons. Thus the engineer who designs based on an experimentally evaluated and calibrated model should increase the safety factors of the study accordingly in order to take into account the fact that the stress field of the test is weaker compared to the actually developed one.

In the particular case of eight-point bending the extreme values of the stresses and strains developed are (at some points of the architrave) almost half the respective values developed if the load is applied uniformly. It is implied therefore that an index should be introduced (a load-correction factor) that would enable the direct comparison between the actual loading states of the architraves (the uniform load corresponding to the own weight of the architrave and structural elements resting on it) and the results obtained from laboratory bending tests.

## **ACKNOWLEDGEMENTS**

The authors are indebted to Mr George Ferentinos (K. Liontos and Associates, ANSYS Channel Partners of Greece) for his valuable comments and his continuous support during the preparation of the numerical models. Also, the assistance of Mr Panagiotis Chatzistergos, PhD student in the Department of Mechanics of the National Technical University of Athens, is gratefully acknowledged. The present study is part of the Master Thesis, in progress, of the second author (E. Ganniari-Papageorgiou).

**REFERENCES**

1. C. Zambas, M. Ioannidou, and A. Papanikolaou, in: *Proc. of the IIC Congress on Case Studies in the Conservation of Stone and Wall Paintings* (The International Institute for Conservation of Historic and Artistic Works, Bologna, 1986), pp. 138-143.
2. M. Ioannidou, and V. Paschalides, in: *Proc. of the 5<sup>th</sup> Int. Symp. for the Restoration of the Acropolis Monuments*, edited by F. Mallouchou-Tufano (Committee for the Preservation of the Acropolis Monuments, Athens, 2002), pp. 291-300.
3. M. Mentzini, in: *Proc. of the 5<sup>th</sup> Int. Symp. for the Restoration of the Acropolis Monuments*, edited by F. Mallouchou-Tufano (Committee for the Preservation of the Acropolis Monuments, Athens, 2002), pp. 233- 242.
4. S. K. Kourkoulis, E. Ganniari-Papageorgiou and M. Mentzini, in: *Proc. of the Int. Conf. on Heritage, Weathering and Conservation-HWC* (Balkema, Rotterdam, 2006) (to appear).
5. V. Paschalides, M. Mentzini, S. K. Kourkoulis and I. Vardoulakis, in: *Proc. of the 1<sup>st</sup> Nat. Conf. of the Greek Association of Mechanical Engineers* (Athens 2004), p. 72. (in Greek).
6. M. Mentzini, A study on the cracks of the epistyles of the peristasis of the Parthenon of Athens, *The Acropolis Restoration News - Anthemion* (Committee for the Preservation of the Acropolis Monuments, Hellenic Ministry of Culture), **6**, (2006), (to appear).
7. I. Vardoulakis, S. K. Kourkoulis, G. E. Exadaktylos and A. Rosakis, in: *Proc. of the Interdisciplinary Workshop "The building stone in monuments*, edited by M. Varti-Mataranga and Y. Katsikis (IGME Publishing, Athens, 2002), pp. 187-210.
8. I. Vardoulakis, G. E. Exadaktylos and S. K. Kourkoulis, Bending of Marble With Intrinsic Length Scales: A Gradient Theory With Surface Energy and Size Effects, *Journal de Physique IV*, **8**, 399-406 (1998).
9. S. K. Kourkoulis, G. E. Exadaktylos and I. Vardoulakis, U-notched Dionysos Pentelicon marble in three point bending: The effect of nonlinearity, anisotropy and microstructure, *International Journal of Fracture*, **98**, 369-392, (1999).
10. S. K. Kourkoulis, M. C. Stavropoulou, I. Vardoulakis and G. E. Exadaktylos, in: *Proc. of the 9<sup>th</sup> Int. Congress on Rock Mechanics*, edited by G. Vouille and P. Berest (Balkema, Rotterdam, 1999), pp. 623-626.